This article has been accepted for publication in a future issue of this journal, but has not been fully edited. Content may change prior to final publication. Citation information: DOI 10.1109/TNS.2019.2939355, IEEE Transactions on Nuclear Science

SOI Thin Microdosimeters for High LET Single Event Upset Studies in Fe, O, Xe and Cocktail Ion Beam Fields

Benjamin James, Linh T. Tran, David Bolst, Stefania Perrachi, Jeremy A. Davis, Dale A. Prokopovich, Susanna Guatelli, Marco Petasecca, Michael Lerch, Marco Povoli, Angela Kok, Marc-Jan Goethem, Mitchell Nancarrow, Naruhiro Matsufuji, Michael Jackson and Anatoly B. Rosenfeld

Abstract **– The response of a 5 µm thin silicon on insulator (SOI) 3D microdosimeter was investigated for single event upset applications by measuring the LET of different high LET ions. The charge collection characteristics of the device was performed using the Ion Beam Induced Charge collection (IBIC) technique with 3 and 5.5 MeV He^{2+} ions incident on the microdosimeter. The microdosimeter was irradiated with ^{16}O, ^{56}Fe and ^{124}Xe ions and was able to determine the LET within 5% for most configurations apart from ^{124}Xe. It was observed that on average, measured LET was 12% lower for 30 MeV/u ^{124}Xe ion traversing through different thickness Kapton absorbers in comparison to Geant4 simulations. This discrepancy can be partly attributed to uncertainties in the thickness of the energy degraders and thickness of the SOI layer of the devices. The effects of overlayer thickness variation is not easy observed for ions with much lower LET as O and Fe. Based on that it is difficult to make conclusion that plasma effect is observed for 30 MeV/u ^{124}Xe ions and further research to be carried out for ion with LET higher than 12 MeV/µm.**

I. INTRODUCTION

Single Event Effects (SEE) occur in microelectronics when highly energetic particles strike sensitive regions of a microelectronic circuit. SEE events can cause four possible outcomes: no observable effect, disruption of circuit operation, change in logic state or permanent damage to the device or integrated circuit [1]. One of the most common environments in which these effects occur is deep space, where a significant number of high energy heavy ions are observed. In these environments, the linear energy transfer (LET) spectrum should be characterised and monitored due to the adverse effects on human health as well as electronic components. This is especially important within the interior of a spacecraft. As heavy ions pass through shielding materials, the energy of such ions is significantly reduced, and can also produce secondary particles. Lower energy ions can have very high LET, which can cause both significant biological damage and radiation damage in microelectric circuits.

Due to the potential of biological and electrical damage in space radiation environment it is important to be able to monitor the incident radiation field of any mix of particles Because size and weight are important considerations in space, it is preferable to have a light and compact detector design.

When a heavy ionizing particle strikes a detector, it creates a dense column of electron–hole pairs, which is considered as plasma if the Debye length is small compared with the column dimensions [3]. This electron-hole pair column serves to reduce the amount of charge collected within the detector due to charge recombination. This occurs as the electric field generated by the applied bias cannot penetrate the high-density cloud of electron-hole pairs formed inside the column. This allows the charge carriers to diffuse laterally within the plasma track. With increasing lateral charge diffusion, the amount of recombination within the detector can be seen to increase. Due to the presence of heavy ionising particles in space it is important that detectors used for monitoring are radiation hard, for both accuracy and lifetime of the device.

Previous work which used a thin SOI microdosimeter (10 µm thick sensitive volume) to measure the LET of different low energy ions showed no presence of plasma effects, with

Manuscript received. This research was supported by the Australian Government through the Australian Research Council's Discovery Projects funding scheme (projects DP 170102273 and DP170102423). This work was supported by computational resources provided by the Australian Government through the Raijin cluster under the National Computational Merit Allocation Scheme. The authors thank all collaborators in the 3D-MiMiC project, funded by the Norwegian Research Council via the NANO2021 program. European Space Agency (ESA) with a grant "Tissue equivalent crew dosimeter based on novel 3D Si processing".

B. James, L. T. Tran, D. Bolst, S. Peracchi, J. Davis, S. Guatelli, M. Petasecca, M. Lerch, M. Nancarrow; A. B. Rosenfeld are with the Centre for Medical Radiation Physics, University of Wollongong, NSW, 2522, Australia (email: bj197@uowmail.edu.au; tltran@uow.edu.au; db001@uowmail.edu.au; sp009@uowmail.edu.au; jeremyd@uow.edu.au; susanna@uow.edu.au; marcop@uow.edu.au; mlerch@uow.edu.au; anatoly@uow.edu.au).

D. A. Prokopovich is with the NSTLI Nuclear Stewardship Platform, Australian Nuclear Science and Technology Organisation (ANSTO), Lucas Heights, NSW 2234, Australia (email: dale.prokopovich@ansto.gov.au).

M. Povoli and A. Kok are with SINTEF, Norway (email: marco.povoli@sintef.no; angela.kok@sintef.no)

Marc-Jan Goethem is with KVI - Center for Advanced Radiation Technology, University of Groningen, Netherlands (e-mail: vgoethem@kvi.nl)

N. Matsufuji is with National Institutes for Quantum and Radiological Science and Technology, Chiba, Japan (e-mail: matsufuji.naruhiro@qst.go.jp).

Michael Jackson is with the University of New South Wales, Sydney, NSW 2052, Australia (e-mail: Michael.Jackson2@health.nsw.gov.au).

This article has been accepted for publication in a future issue of this journal, but has not been fully edited. Content may change prior to final publication. Citation information: DOI 10.1109/TNS.2019.2939355, IEEE Transactions on Nuclear Science

LETs reaching up to approximately 7 MeV/µm [2]. The aim of this work was to study the applicability of a new generation, thinner silicon microdosimeter for higher LET ion measurements.

II. METHOD

A. *Detector Structures*

The Mushroom microdosimeter structures used in this work are the second generation of devices developed by the Centre for Medical Radiation Physics (CMRP), University of Wollongong in collaboration with SINTEF MiNaLab, Oslo, Norway. With respect to the previous generation, several modifications were adopted to simplify the fabrication process to allow for improved electrical characteristics with higher reliability. In the first generation, major issues were discovered with the metal line connections traversing over regions with high topography, where a large number of disrupted connections were observed, resulting in many sensors having multiple sensitive volumes not connected [4]. In this second generation, the topography of the front surface was reduced significantly to increase the robustness of the metal connections. The planarization process in the second generation was achieved by etching the polysilicon regions on the surface of the device.

Fig. 1a shows simplified schematics illustrating sensitive volume geometry of a trenched planar mushroom microdosimeter. Fig. 1b shows an SEM image of the device.

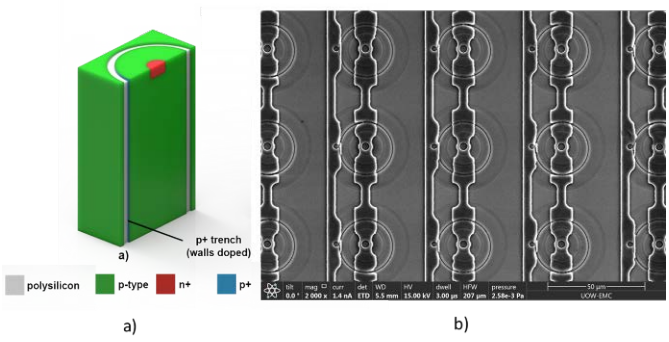

Figure 1: a) Simplified schematics illustrating sensitive volume geometry of a trenched planar structure and b) scanning electron microscope (SEM) image of the mushroom micodosimeter.

The second issue observed in the first generation of planar trenched structure of the mushroom microdosimeter was the build-up charge in the oxide layer surrounding the SVs after irradiations [4]. In this new generation of microdosimeter, the p-stop implantation is connected to the p+ doping of the cylindrical trench (NO-GAP configuration). This topology can provide charge collection conformal to the SV when the devices are irradiated with high intensity beams, i.e. completely avoiding the effect of positive charge build-up in PSTOP oxide leading to charge collection from outside of the SV through the bridges between SVs [2].

In this work 5 µm thin active layer microdosimeters with different sizes and pitches of SVs were tested and investigated. The different diameters of the SV designs include 18 µm, 30 µm and 50 µm with distances between core to core of adjacent SVs (pitch) of 30 or 50 µm. Fig. 2 shows the cross section of the 5 µm thin and 18 µm diameter microdosimeter which was obtained using scanning electron microscope after milling the device using a focused ion beam at the Electron Microscopy Centre, Australian Institute for Innovative Materials (AIIM) at UOW. It can be seen that a trench, which reaches the bottom of the active layer of silicon, was etched into the silicon which is filled with polysilicon. This trench acts to isolate the charge sharing between adjacent SVs.

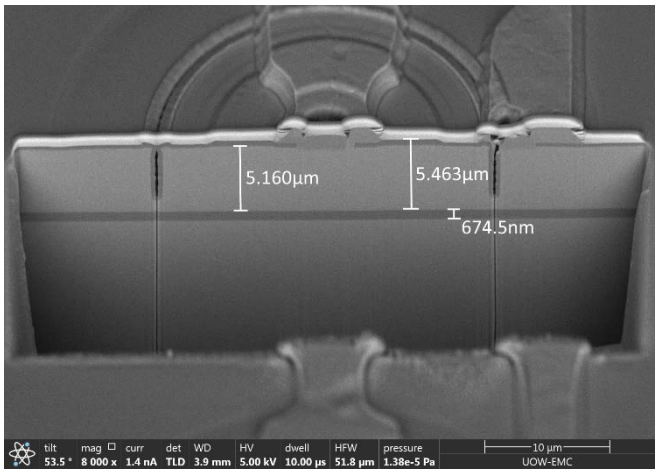

Figure 2: Cross-section image of the 5 µm thin mushroom microdosimeter.

B. *Charge Collection Study*

The charge collection properties of the new generation of mushroom microdosimeter was studied in detail using the ion beam induced charge collection technique (IBIC) at the 6 MV accelerator SIRIUS, located at the Centre for Accelerator Science (CAS) facility at Australian Nuclear Science and Technology Organisation (ANSTO) [5],[6].

The IBIC measurements utilized a microbeam of 3 MeV and 5.5 MeV He^{2+} ions which were raster scanned over the surface of the sample. The spot size of the microbeam is approximately 1 µm. Energy deposited in the microdosimeter was measured using an AMPTEK A250 charge sensitive preamplifier and a Canberra 2025 Shaping Amplifier with 1 µs shaping time. The signal corresponding to the beam's position “x” and “y” as well as the energy deposited “E” for each event was processed into an event-by-event list mode file. The data was processed into median charge collection image maps for spatial correlation of the energy deposition of the scanned area [2]. The energy calibration was performed using a calibrated pulse generator, which was calibrated with a 300 µm thick fully depleted planar silicon Hamamatsu PIN

This article has been accepted for publication in a future issue of this journal, but has not been fully edited. Content may change prior to final publication. Citation information: DOI 10.1109/TNS.2019.2939355, IEEE Transactions on Nuclear Science

photodiode with 100% Charge Collection Efficiency (CCE) in response to 3 MeV and 5.5 MeV He^{2+} ions.

C. *Charge Collection Efficiency*

An approximate charge collection efficiency (CCE) value was calculated using the peak energy determined from IBIC and the peak value taken from a Geant4 simulation spectrum. Detailed detector geometry and overlayers thicknesses taken from SEM image were included in Geant4 simulation.

$$CCE(\%) = \frac{E_{IBIC}}{E_{Geant4}}\ x\ 100$$

D. *HIMAC Irradiation*

In order to study the response of this new microdosimeter for different energy ranges of heavy ions which exist in deep space environments, an experiment was carried out with 400 MeV/u ^{16}O ions and 500 MeV/u ^{56}Fe ions at the Heavy Ion Medical Accelerator in Chiba (HIMAC), located at the National Institute of Radiological Sciences (NIRS) in Japan.

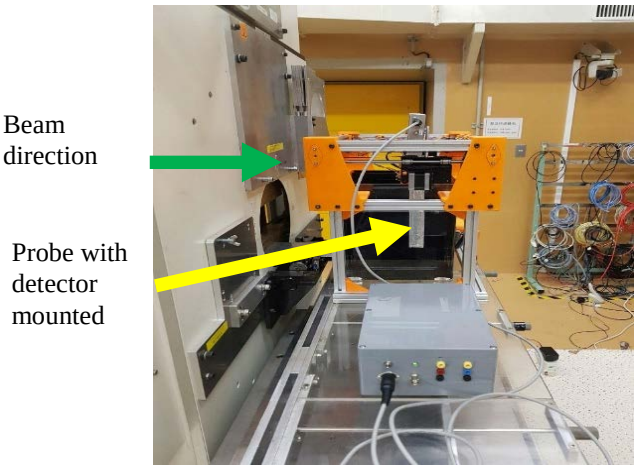

Figure 3: The remote control movable platform holding the detector mounted on the MicroPlus probe in a water phantom, connected to power supply box.

Mono-energetic ^{16}O and ^{56}Fe ions with initial energies of 400 MeV/u and 500 MeV/u, respectively were used in this experiment to irradiate the microdosimeter. The mushroom microdosimeters were connected to a low noise spectroscopy-based readout circuit (also called a MicroPlus probe). The probe was inserted into a water proof sheath and then placed in a water tank, shown in Figure 3. The MicroPlus probe measured at different depths in water along the central axis of the 400 MeV/u ^{16}O and 500 MeV/u ^{56}Fe ion beams. We define the quantity LET_{MCA}, calculated from the experiment and Geant4 simulation. This differs from the LET provided by SRIM [7], which is the theoretical energy lost by the ion in silicon. LET_{MCA} is defined as the energy deposition peak of the primary beam obtained in the multichannel analyser (MCA) spectrum divided by the SOI active layer thickness of the microdosimeter. The ion energy for each experimentally obtained LET_{MCA} value corresponds to the energy of the ion after traversing water and over layers of microdosimeter calculated using Geant4. In the simulation, the ion energy was tuned to 493 MeV/u for Fe ions and 394 MeV/u for O ions to match the observed range in the experiment.

E. *KVI Irradiation*

The response of the new microdosimeter was also studied in mixed low energy ions (cocktails) at KVI - Center for Advanced Radiation Technology, Netherlands. Oxygen and Xenon ion beams were produced by the Advanced Electron Cyclotron Resonance (AECR) ion-source and accelerated to approximately 30 MeV/u by the AGOR cyclotron. The ions were transported in vacuum to the irradiation setup which is in air. The 50 µm aramid vacuum window was located 79 mm upstream of the detectors. The beam intensity was reduced such that the count rate of the silicon detectors would not produce pile-up. A selection of degrader materials were inserted using a carousel of 8 degrader foils which is located just in front of the detector (Fig. 4).

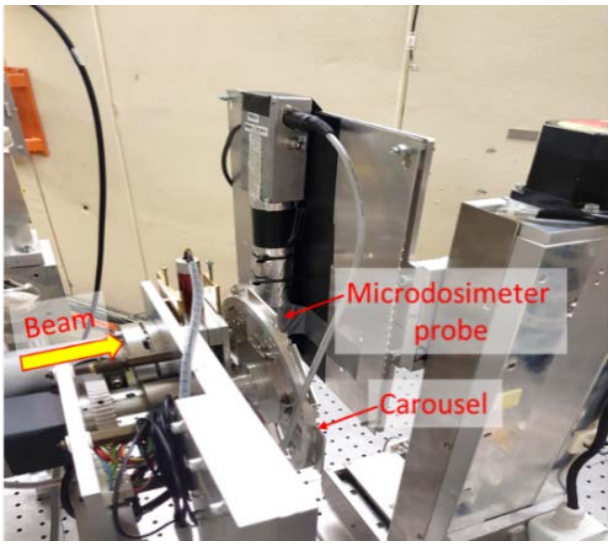

Figure 4: Experimental setup at KVI

F. *Geant4 Modelling*

The two configurations used to irradiate the microdosimeter at NIRS and KVI were modelled using the Geant4 (version 10.02p3) toolkit [8], [9]. For the HIMAC beamline, an existing simulation which has been previously described extensively and validated in Ref. 10 was used. Briefly, the beamline consists of a pencil beam which is shaped by a pair of wobbler magnets to shape the beam into a circular shape with a diameter of 100 mm at iso-centre. After passing through the pair of wobbler magnets the dose uniformity of beam is improved by passing through scatterer filters. For the ^{16}O ion beam the scatterer filter was 0.91 mm thick tantalum while for the ^{56}Fe ion consisted of 1.6 mm of lead and 0.215 mm of tantalum. After the beam passes the

This article has been accepted for publication in a future issue of this journal, but has not been fully edited. Content may change prior to final publication. Citation information: DOI 10.1109/TNS.2019.2939355, IEEE Transactions on Nuclear Science

scatter filter its neutron contribution is reduced by passing through a neutron shutter and is then shaped by a series of collimators, with the final collimation being performed by a pair of moveable X-Y brass collimators 5 cm thick.

The KVI beamline was modelled with the beam generated before the vacuum window, between the window and surface of the detector there was 79 mm of air, with the degrader material being 30 mm in front of the detector.

The Mushroom microdosimeter was accurately modelled in Geant4, with overlayers taken into account. For an extensive description of the modelling of the mushroom microdosimeter design in Geant4, readers are directed towards ref. [11]. Ref. 11 performed a validation study of the first generation air-trenched microdosimeter in heavy ion therapy. Although the work discussed in this paper uses a second generation device, the method discussed for the first generation device is similar.

The Geant4 Low Energy Physics Package, based on Livermore data libraries was selected to describe the electromagnetic interactions of particles. The threshold of production for e-, e+ and ɣ was set to 250 eV, which is the lower limit of validity of this physics model [12], [13]. The Geant4 QGSP BIC HP (high-precision) physics list was selected to model the hadronic physics processes.

III. RESULTS

A. *Charge Collection Study*

Fig. 5 shows the MCA spectra obtained at 0 V and 10 V in response to 3 MeV He^{2+} ions for the 5 µm Mushroom microdosimeter, using the IBIC technique. The energy peak was observed at 1163 keV which corresponds correctly to the expected energy deposition of 1150 keV in 5 µm thin silicon with 1.2 µm Al and 400 nm oxide calculated using a Geant4 simulation. It can be seen that at 0V the detector is almost completely depleted, with only a 3% difference in CCE between 0 and 10V. Overall the trenched planar structure has been shown in previous work to have a CCE of 96% [4].

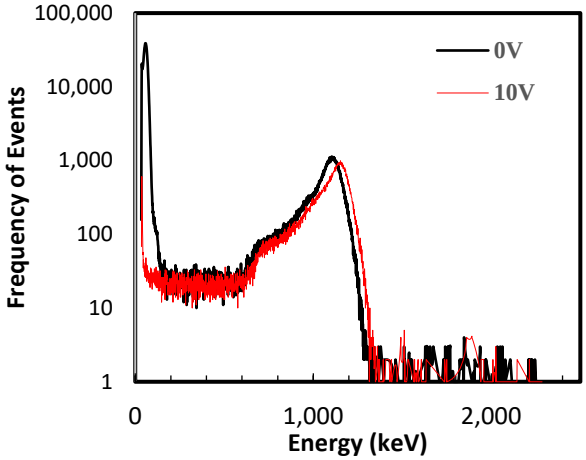

Figure 5: MCA spectra obtained with the 5 µm thin microdosimeter at 0V and 10V in response to 3 MeV He^{2+} ions.

Fig. 6 shows the median energy map of the full array of sensitive volumes. It can be clearly seen that 100% yield was obtained in this generation of Mushroom microdosimeter. Each SV has a diameter of 30 µm, with a pitch of 50 µm between SVs. It can be seen that each of the sensitive volumes has very uniform charge collection and well-defined volume shapes. Very low energy charge was observed in a narrow region surrounding each SV due to the trench wall filled with polysilicon. Furthermore, no charge collection can be seen within the connecting regions between sensitive volumes when the detector is biased.

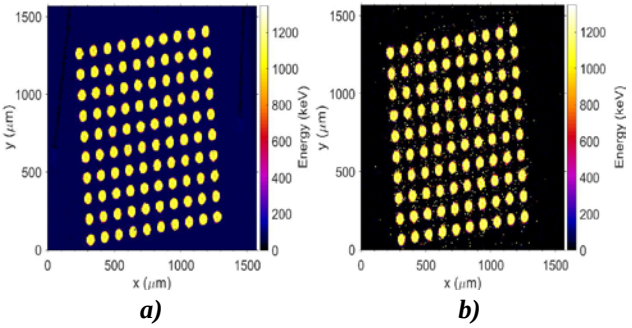

Figure 6: Median energy map of 5 µm thin mushroom microdosimeter in response to 3 MeV He^{2+} ion at **a)** 0 and **b)** 10 V

The response of the microdosimeter to a 5.5 MeV He^{2+} scanning microbeam when the detector is biased at 10V is shown in Fig. 7. The median energy map shows four SVs collecting charge individually, there is some random events outside the SVs but these are related to noise in the electronics, meaning that no charge collection was observed from outside the SV. Fig. 8 show the MCA spectra and windowed median energy maps obtained in response to the He^{2+} ions. The energy deposited by the He^{2+} ions crossing the SVs produces a peak at approximately 760 keV.

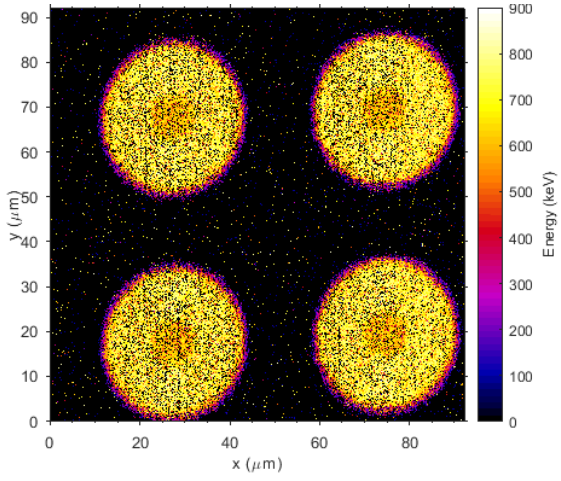

Figure 7: Median Energy map of mushroom microdosimeter showing 4 cells at 10V in response to a 5.5MeV He^{2+} beam.

Comparing the experimental peak obtained using IBIC, with the simulated average peak energy of 760 keV. It can be seen that the CCE within the SV (not including the core) is almost exactly 100%.

This article has been accepted for publication in a future issue of this journal, but has not been fully edited. Content may change prior to final publication. Citation information: DOI 10.1109/TNS.2019.2939355, IEEE Transactions on Nuclear Science

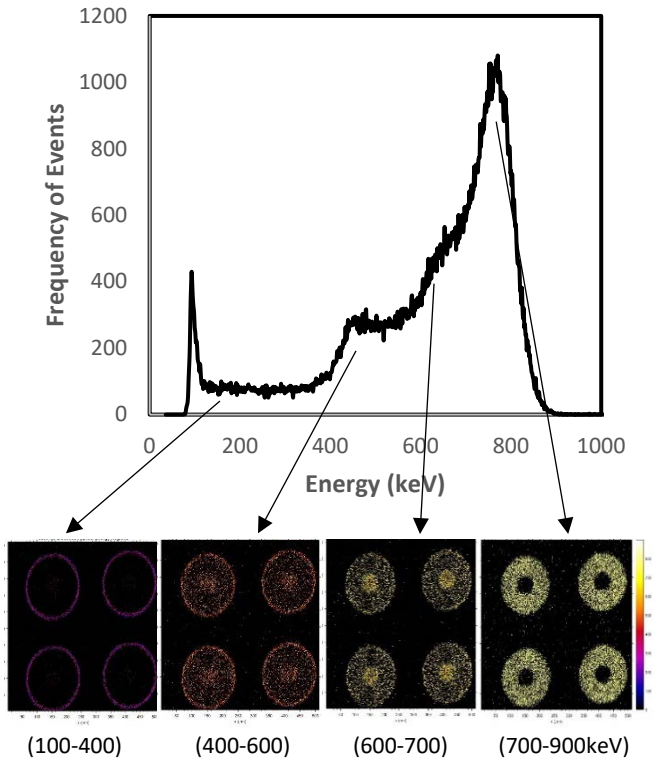

Figure 8: MCA spectra of IBIC with associated energy windowing

Low energy events in the spectrum from 100-400 keV occur in the border ring of the SV next to the polysilicon trench (~1 µm width), due to p+ doping going into the inner side wall of the cylindrical SV. Charge collection within the SVs is very uniform except for within the n+ planar core. The energy window of 400-600 keV and 600-700 keV in the MCA spectrum, shows that there is a deficit of collected charge produced by He^{2+} ions in the planar core. Calculating the CCE with respect to the frequency of events, it can be seen that on average the CCE within the planar core is approximately 84%.

B. *LET measurements of SOI microdosimeter for a 500 MeV/u ^{56}Fe and 400 MeV/u ^{16}O beam*

Fig. 9 shows a comparison of LET and LET_{MCA} values in silicon for Fe ions of different energies in silicon calculated using SRIM, Geant4 and experiment using the 5 µm thin Mushroom microdosimeters. The experimental results for Fe match values from SRIM reasonably well. The values of LET_{MCA}, measured by the microdosimeter, are slightly lower compared to the theoretical values calculated by SRIM. Part of the difference can be attributed to delta electrons produced along the ion track which do not contribute to the LET_{MCA} but is included in the unrestricted LET value as energy lost to the medium as calculated using SRIM. Comparing to Geant4, it can also be seen that Geant4 gives slightly lower values compared to SRIM, giving excellent agreement with experimental results.

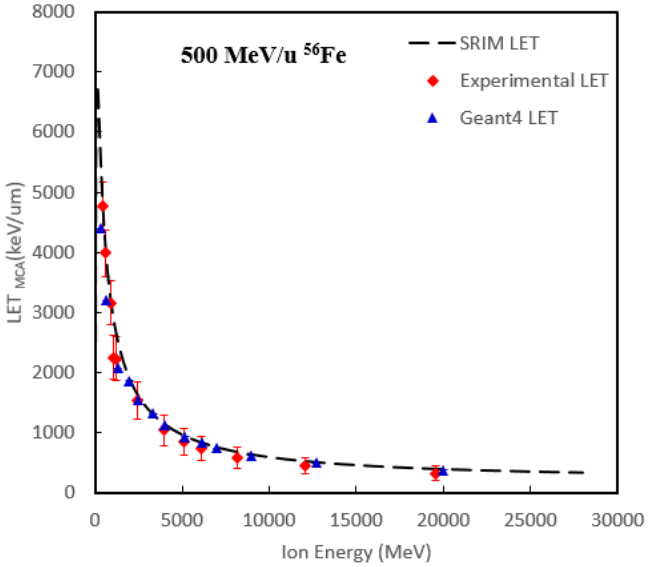

Figure 9: LET_{MCA} measurements by SOI Mushroom microdosimeters at different depths in water for 500 MeV/u ^{56}Fe in comparison with SRIM and Geant4 data.

Similarly to Fe ions, the LET_{MCA} values obtained with the microdosimeter agreed well with the calculated values using SRIM. A slight difference between the measured LET_{MCA} and LET calculated using SRIM at lower ion energy (less than 500 MeV) of O ions could be due to the positioning of the microdosimeter at the last few millimetres of the Bragg peak where the LET of ions is significantly increasing and even submillimetre uncertainty will lead to significant error in ion energy (Fig. 10). These results demonstrated that the SOI Mushroom microdosimeter is suitable for LET measurements of different ion energies.

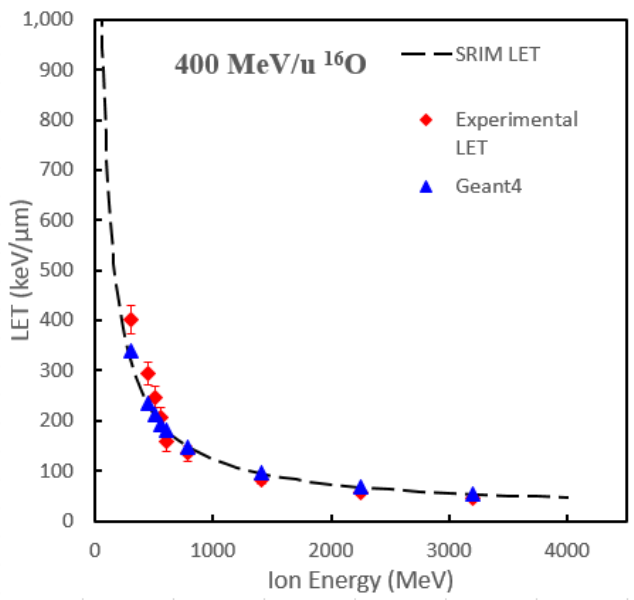

Figure 10: LET_{MCA} measurements by SOI Mushroom microdosimeters at different depths in water for 400 MeV/u ^{16}O in comparison with SRIM and Geant4 data.

This article has been accepted for publication in a future issue of this journal, but has not been fully edited. Content may change prior to final publication. Citation information: DOI 10.1109/TNS.2019.2939355, IEEE Transactions on Nuclear Science

C. *KVI Measurements – Oxygen*

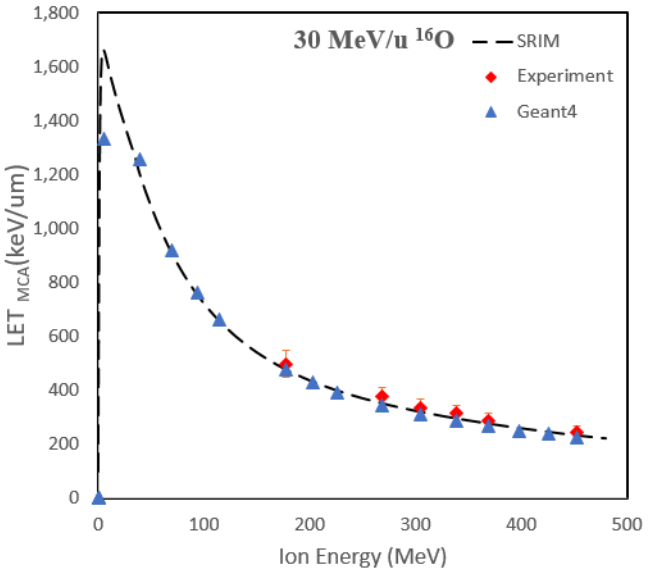

Figure 11: LET_{MCA} measurements by SOI Mushroom microdosimeters with different thickness Aluminium absorbers for 30 MeV/u ^{16}O in comparison with SRIM and Geant4 data.

Figure 11 shows a comparison of LET and LET_{MCA} values in silicon for 30 MeV/u Oxygen ions of different energies in silicon, produced by different thicknesses of Aluminium absorbers for SRIM, Geant4 and experimental results.

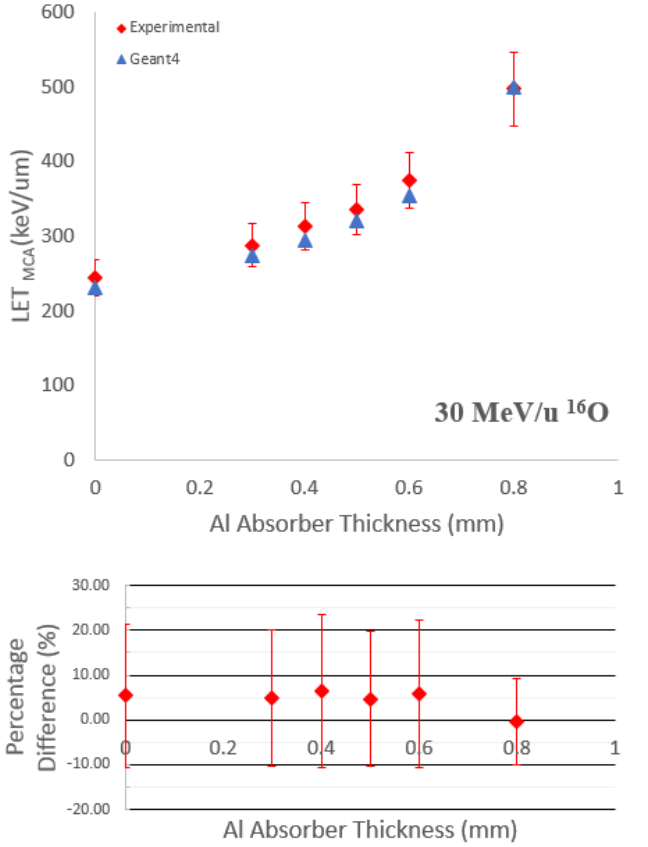

Figure 12: Percentage difference of experimentally measured LET_{MCA} of ^{16}O in comparison to Geant4 predicted for different thicknesses of Aluminium absorbers.

There is good agreement between experimental results and both SRIM and Geant4 within the uncertainty. The uncertainty of the LET_{MCA} (vertical error bars) was calculated based on the uncertainty in the thickness of the SOI active layer (±0.5 µm).

Figure 12 shows a comparison of the LET_{MCA} values obtained from experimental results and Geant4 for Oxygen. For most absorbers there is approximately a 5% higher response from the experimental data. This corresponds to a difference in peak value of approximately 15-20 keV. The thickest absorber (0.8mm Al) shows good agreement between experimental and Geant4 results, this can be attributed to reduced uncertainty in the thickness of Al used.

D. *KVI Measurements – Xenon*

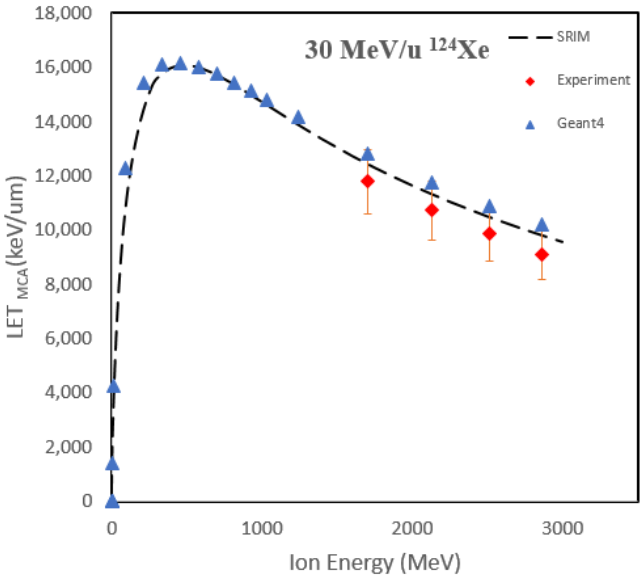

Figure 13: LET_{MCA} measurements by SOI Mushroom microdosimeters with different thickness of Kapton absorbers for 30 MeV/u ^{124}Xe in comparison with SRIM and Geant4 data.

Figure 13 shows a comparison of LET and LET_{MCA} values in silicon for Xenon ions of different energies in silicon, produced by different thicknesses of thin Kapton absorber, for SRIM, Geant4 and experimental results. There is good agreement between Geant4 and SRIM, however experimental results show a significant under response. This may be contributed from uncertainties in the thickness of the SOI as half a µm of silicon will result in huge discrepancy in the energy loss due to extremely high LET of ^{124}Xe ions. It could also be due to plasma effect within the detector, causing recombination and therefore reducing the total charge collected. While this has not been seen in previous work [2], and in this work with Oxygen and Fe ions, the energy being deposited in the case of Xenon can be an order of magnitude higher, increasing the likelihood of plasma effect occurring. Total energy deposited by Xenon ranged from 46 – 59 MeV in 5 µm, corresponding to LET_{MCA} values of 9.2 – 11.8 MeV/µm, respectively (range of Xe ion of 46 and 59 MeV in silicon is 9.14 and 10.63 µm, respectively).

This article has been accepted for publication in a future issue of this journal, but has not been fully edited. Content may change prior to final publication. Citation information: DOI 10.1109/TNS.2019.2939355, IEEE Transactions on Nuclear Science

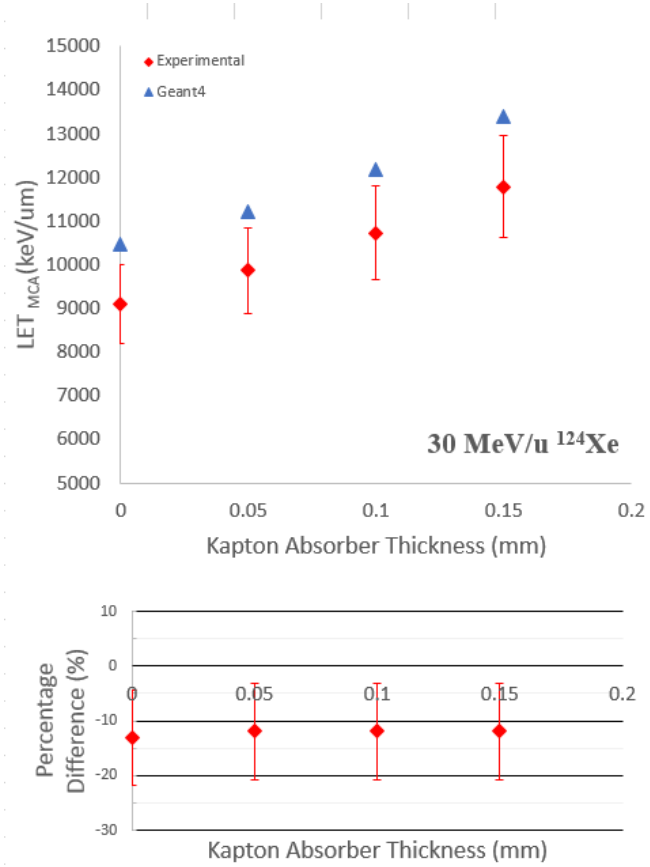

Figure 14: Percentage difference of experimentally measured LET_{MCA} of ^{124}Xe in comparison to Geant4 predicted for different thicknesses of Kapton absorbers.

Figure 14 shows a comparison of the LET_{MCA} values obtained from experimental results and Geant4 for Xenon. For most absorbers there is approximately a 12% lower response from the experimental data. This corresponds to a LET_{MCA} value difference of between 0.8-1.1 MeV/µm.

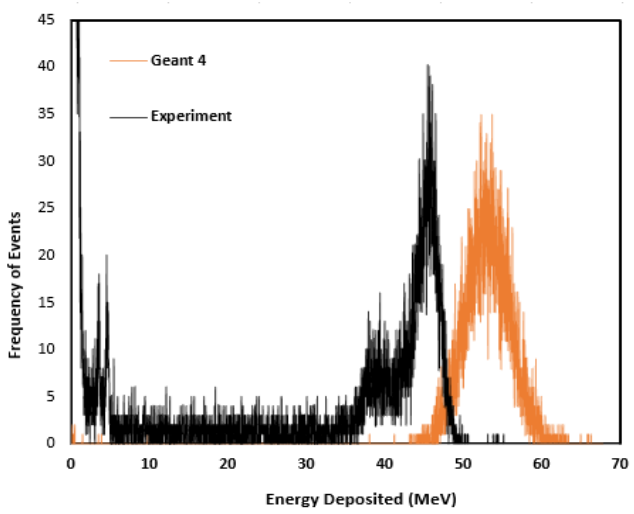

Figure 15: MCA spectra obtained by 5 µm thin SOI Mushroom microdosimeter with no Kapton degrader for 30 MeV/u ^{124}Xe ion, compared to Geant4 simulated spectra.

Comparing experimental MCA data to Geant4 simulated data, the experimental energy deposition spectrum is significantly shifted to the left. Figure 15 compares the MCA spectra obtained experimentally with no Kapton absorber with the same spectrum simulated with Geant4.

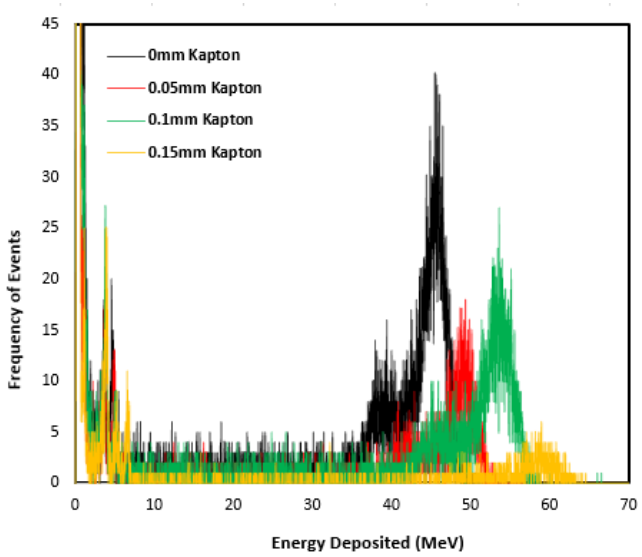

Figure 16: MCA spectra obtained by 5 µm thin SOI Mushroom microdosimeters with different thicknesses of Kapton degrader for 30 MeV/u ^{124}Xe ion.

It can be seen that with no absorber, the main Xenon peak was observed at approximately 46 MeV and the small peak was seen at approximately 4.6 MeV which was due to the contamination of Oxygen ion in the beam. In comparison, the Geant4 spectra has a peak at approximately 52 MeV. An interesting feature in the experimental spectrum is the secondary Xenon peak, which is due to the lower CCE in the n+ planar core of the device as observed with IBIC (Fig. 8) and emphasized due to the high LET of Xenon ions. As Geant4 only simulates physical processes, events caused by lower charge collection are not present in the Geant4 spectrum, hence no secondary peak is observed. The energy of this secondary peak is approximately 39.3 MeV, corresponding to 84% of the primary peak energy, giving good agreement with the CCE efficiency of the planar core found using IBIC.

Fig. 16 shows the response of the microdosimeter in a Xe ion beam with different thicknesses of Kapton absorbers of: 0 mm, 0.05 mm, 0.1 mm and 0.15 mm. With 0.05 mm and 0.1 mm Kapton, the Xe peaks shifted to the right due to higher LET Xe ions straggling in Kapton and deposited more energy into the silicon detector. With 0.15 mm Kapton, the Xe almost fully stopped in the detector and very high LET ions deposited approximately 52 MeV into silicon.

IV. CONCLUSION

The responses of the second generation Mushroom SOI microdosimeters with thinner SVs than first generation, developed by CMRP were investigated with a wide range of ions namely Fe, O, Xe, cocktails. For O and Fe ions, the experimental results obtained from measurements in water at

different depths agreed reasonably well with SRIM and Geant4 simulation. The LET_{MCA} values of O and Fe ions are slightly less than theoretical calculated LET using SRIM at higher energies due to delta electrons produced along the ion track which do not contribute to the LET_{MCA} but is included in SRIM calculation. For lower energies of O ions measured LET_{MCA} is about 5-7% higher than predicted by SRIM or Geant4 because the range of ions is comparable with SOI layer thickness and deposited energy along the ion path in SV is increasing, leading to a higher apparent LET. It was also observed that on average, measured LET was 12% lower for 30 MeV/u ^{124}Xe ion traversing through different thickness Kapton absorbers in comparison to Geant4 simulations. Considering error bars based on SOI thickness spreading provided by manufacturing, agreement is reasonable. While Geant4 simulation of deposited energy (Fig 14) was calculated for 5.16 µm thickness of SOI measured by SEM (Fig 2.) for SV in a particular device from one of the SOI wafer it is not guaranteed that the same thickness was in the device used for the ^{124}Xe experiment as manufacturer guarantee thickness of SOI layer ± 0.5 µm. For example, considering thickness of the SOI layer as 4.7 µm will provide perfect agreement in LET predicted by SRIM for ^{124}Xe ions with energy 30 MeV/u. Effect of slight possible variation of SOI layer thickness is not easily observed for ions with much lower LET as O and Fe. Based on that it is impossible to make conclusion that plasma effect is observed for 30 MeV/u ^{124}Xe ions and further research to be carried out for ion with LET higher than 12 MeV/µm. It has been demonstrated that the developed 5 µm SOI mushrooms can measure in a mixed ion field with LET up to 12 MeV/µm in silicon. Build up charge effects within the SiO_2 has been addressed in this version, no significant radiation damage was observed after irradiation with high LET ions.

ACKNOWLEDGEMENTS

We would like to thanks Australian Research Council (ARC) for support of this research with a Discovery Project Grant “Development of radiation detectors to better understand ion interactions” (DP 170102273) and European Space Agency (ESA) with a grant “Tissue equivalent crew dosimeter based on novel 3D Si processing” Contract No. 4000112670/14/NL/HK. The authors wish to acknowledge the National Collaborative Research Infrastructure Strategy (NCRIS) funding provided by the Australian Government for this research. The authors would like to acknowledge Dr. Andrew See at the UNSW ANFF node for their packaging work as well as Prof. Elena Pereloma and her electron microscopy team at the Australian Institute for Innovative Materials, University of Wollongong for their excellent imaging work.

REFERENCES

[1] P. Dodd, L. Massengill, “Basic Mechanisms and Modeling of Single-Event Upset in Digital Microelectronics”, *IEEE Trans Nucl Sci*, vol. 50, no. 3, June 2003.

[2] B. James, L. T. Tran, J. Vohradsky et al., "SOI Thin Microdosimeter Detectors for Low-Energy Ions and Radiation Damage Studies," *IEEE Trans Nucl Sci*, vol. 66, no. 1, pp. 320-326, Jan. 2019.

[3] R. Williams and E. M. Lawson, “The plasma effect in silicon semiconductor radiation detectors”, *Nucl. Instrum. Meth.*, vol. 120, pp. 261-268, 1974

[4] L. T. Tran, L. Chartier, D. Bolst, et al., “Thin silicon microdosimeter utilizing 3D MEMS technology: Charge collection study and its application in mixed radiation fields,” *IEEE Transactions on Nuclear Science*, vol. 65, no. 1, pp. 467–472, 2017

[5] Z. Pastuovic, R. Siegele, D. Cohen, et al., “The new confocal heavy ion microprobe beamline at ANSTO,” *Nucl. Instrum. Meth., Phys. Res. B*, vol. 404, pp. 1 – 8, Aug 2017.

[6] Z. Pastuovic, J. Davis, L.T. Tran, et al, “IBIC microscopy – The powerful tool for testing micron – Sized sensitive volumes in segmented radiation detectors used in synchrotron microbeam radiation and hadron therapies,” *Nucl. Instrum. Meth., Phys. Res. B*, vol. 458, pp. 90 – 96, 2019

[7] J. F. Ziegler, M. D. Ziegler, J. P. Biersack, et al, “SRIM - The stopping and range of ions in matter,” Nucl. Instrum.Methods Phys. Res. B., vol. 268, no. 11–12, pp. 1818–1823, Jun. 2010.

[8] S. Agostinelli, J. Allison, K. Amako, et al., “Geant4a simulation toolkit,” *Nucl. Instrum. Meth., Phys. Res. A*, vol. 506, no. 3, pp. 250 – 303, July 2003.

[9] J. Allison, K. Amako, J. Apostolakis, et al., “Geant4 developments and applications,” IEEE Trans Nucl Sci, vol. 53, no. 1, pp. 270– 278, Feb 2006.

[10] D. Bolst, L. T. Tran, S. Guatelli, N. Matsufuji and A. B. Rosenfeld, “Modelling the Biological Beamline at HIMAC using Geant4,” J. Phys. Conf. Ser., vol 1154, pp. 012003, 2019, doi: 10.1088/1742-6596/1154/1/012003

[11] D. Bolst, S. Guatelli, L. T. Tran, L. Chartier, J. Davis, D. A. Prokopovich, A. Pogossov, M. I. Reinhard, M. Petasecca, M. L. F. Lerch, N. Matsufuji , M. Povoli, A. Summanwar, A. Kok, M. Jackson and A. B. Rosenfeld, “Validation of Geant4 for silicon microdosimetry in heavy ion therapy”, Phys Med Bio, (In press)

[12] S. Chauvie, Z. Francis, S. Guatelli, et al., “Geant4 physics processes for microdosimetry simulation: Design foundation and implementation of the first set of models,” *IEEE Trans Nucl Sci*, vol. 54, no. 6, pp. 2619–2628, Dec 2007.

[13] K. Amako, S. Guatelli, V. N. Ivanchenko, et al., “Comparison of geant4 electromagnetic physics models against the nist reference data,” *IEEE Trans Nucl Sci*, vol. 52, no. 4, pp. 910–918, Aug 2005.